Computational and Structural Biotechnology Journal 19 (2021) 5360–5370

COMPUTATIONAL AND STRUCTURAL BIOTECHNOLOGY JOURNAL

journal homepage: www.elsevier.com/locate/csbj

A rapid CRISPR competitive assay for *in vitro* and *in vivo* discovery of potential drug targets affecting the hematopoietic system

Yunbing Shen [a], Long Jiang [a,1], Vaishnavi Srinivasan Iyer [a,b,1], Bruno Raposo [a], Anatoly Dubnovitsky [a,c], Sanjaykumar V. Boddul [a], Zsolt Kasza [a], Fredrik Wermeling [a,*]

[a] Department of Medicine Solna, Center for Molecular Medicine, Karolinska University Hospital and Karolinska Institutet, Stockholm, Sweden
[b] School of Physical and Mathematical Sciences, Nanyang Technological University, Singapore
[c] Science for Life Laboratory, Department of Medicine Solna, Karolinska Institutet, Stockholm, Sweden

ARTICLE INFO

Article history:
Received 10 May 2021
Received in revised form 29 August 2021
Accepted 16 September 2021
Available online 20 September 2021

Keywords:
CRISPR
Sequence analysis
Drug target discovery
Cell assay
In vivo model
Hematopoiesis
Immune cells
Leukemia

ABSTRACT

CRISPR/Cas9 can be used as an experimental tool to inactivate genes in cells. However, a CRISPR-targeted cell population will not show a uniform genotype of the targeted gene. Instead, a mix of genotypes is generated - from wild type to different forms of insertions and deletions. Such mixed genotypes complicate analysis of the role of the targeted gene in the studied cell population. Here, we present a rapid and universal experimental approach to functionally analyze a CRISPR-targeted cell population that does not involve generating clonal lines. As a simple readout, we leverage the CRISPR-induced genetic heterogeneity and use sequencing to identify how different genotypes are enriched or depleted in relation to the studied cellular behavior or phenotype. The approach uses standard PCR, Sanger sequencing, and a simple sequence deconvoluting software, enabling laboratories without specific in-depth experience to perform these experiments. As proof of principle, we present examples studying various aspects related to hematopoietic cells (T cell development *in vivo* and activation *in vitro*, differentiation of macrophages and dendritic cells, as well as a leukemia-like phenotype induced by overexpressing a proto-oncogene). In conclusion, we present a rapid experimental approach to identify potential drug targets related to mature immune cells, as well as normal and malignant hematopoiesis.

1. Introduction

1.1. Clustered regularly interspaced short palindromic repeats (CRISPR)

CRISPR has been developed from its natural prokaryotic origins into a set of molecular biology tools that can be used to modify genes in eukaryotic cells [1–4]. In its most simple form, a CRISPR experiment involves delivering a single guide RNA (sgRNA), with specificity for the gene of interest, together with the endonuclease Cas9 into the nucleus of the studied cell [5], which, if designed correctly, has a good chance of resulting in the inactivation of the gene.

Experiments comparing pairs of cell lines or animals that differ at one specific genetic region, for example being wild type (WT) and knockout (KO) for a gene of interest, is a powerful approach that is extensively used to identify the role of the gene for a studied phenotype. Due to its simplicity, CRISPR is playing an increasingly important role in this regard, generating cell lines and animal models with specific genetic modifications. However, the mutation spectrum created in a CRISPR-targeted cell population is not uniform. Instead, both unmodified (WT), as well as insertions and deletions (InDels) of different sizes, are typically generated when the Cas9 induced DNA damage is repaired by the error-prone non-homologous end-joining pathway [6–7]. The genetic heterogeneity makes it difficult to directly analyze the role of a targeted gene, and researchers often generate clonal lines with defined mutations from the modified cell population. It is, however, not feasible to generate clonal lines from many cell types, including most primary cell populations.

Several approaches have been developed to evaluate the genetic heterogeneity in a CRISPR-targeted cell population. These include next-generation sequencing (NGS) platforms [8–10], approaches based on fragment length analysis (FLA) of PCR amplicons, like IDAA (Indel Detection by Amplicon Analysis) [11–12], as well as

* Corresponding author at: Center for Molecular Medicine, L8:03, Karolinska University Hospital, 171 76 Stockholm, Sweden.
E-mail address: fredrik.wermeling@ki.se (F. Wermeling).
[1] Shared authorship.

https://doi.org/10.1016/j.csbj.2021.09.020
2001-0370/

analysis tools like ICE (Inference of CRISPR Edits) [13], and TIDE (Tracking of Indels by DEcomposition) [14] that deconvolute Sanger sequencing data into the frequency of different genotypes found in a sample.

1.2. The hematopoietic system

Hematopoiesis is the essential process where mature immune cells, platelets, and erythrocytes are formed from hematopoietic stem cells (HSCs) located in specific adult bone marrow (BM) niches of higher vertebrates [15–18]. Of importance, malignancies at different developmental stages of the hematopoietic lineage, including leukemia, represent the major cancer types seen in children and adolescents [19], as well as constituting a significant amount of all cancers observed in adults [20].

The concept that the BM contains precursor cells for the adult hematopoietic system was formally proven in the 1950 s by experiments and clinical treatment showing that the transplantation of BM cells into an irradiated host results in the formation of mature immune cells stemming from the donor HSCs [21–22]. BM transplantations are nowadays an integrated part of the clinical practice, including in the treatment of leukemia, but are also extensively used in experimental immunological research. For example, BM cells from mice with different genotypes (e.g. WT and KO for a gene of interest) can be combined and transplanted into an irradiated recipient mouse, generating a "mixed BM chimeric" mouse, where cells of different genotypes can compete. However, accessing or generating mice (or cells) with specific genotypes is time-consuming and expensive. Here, we present an alternative CRISPR-based approach based on genotype competition to study genes affecting the hematopoietic system *in vivo* and *in vitro*.

2. Material and methods

2.1. Mice.

8 to 12 week old, sex- and age-matched mice were used in experiments. All mice were housed in specific pathogen-free conditions with a 12/12-hour light/dark cycle and fed standard chow diet *ad libitum*. All animal experiments were approved by the local Stockholm ethical committee, Sweden. C57BL/6 Cas9 + GFP+ (stock no. 026179, CD45.2 +), and C57BL/6 CD45.1 (stock no. 002014) were acquired from Jackson Laboratory. Additionally, homozygous Cas9 + GFP + CD45.1 + mice (Cas9.1) were generated by crossing C57BL/6 Cas9 + GFP + mice and C57BL/6 CD45.1 mice, and genotyping offspring using flow cytometry to detect GFP and CD45.1.

BM transplantations were performed by i.v. injection of $\sim 10^6$ bone marrow cells into recipient mice irradiated with 900 rad of γ-irradiation 12–24 h earlier. The bone marrow cells were typically electroporated with a sgRNA<2 h before being injected into the recipient mice. To evaluate the mutations of the BM cells, a fraction of the electroporated cells were kept in culture, to allow for the CRISPR event to occur, and sequenced two days later.

2.2. sgRNA and primer design.

The Green Listed software (http://greenlisted.cmm.ki.se/) utilizing the Brie reference library, typically selecting the sgRNA with the highest on-target activity [23], or https://design.synthego.com/#/ were used to design sgRNAs. sgRNAs with stabilizing 2′-O-methyl and phosphorothioate linkages were ordered from Sigma-Aldrich or Synthego. The geneMANIA plugin for Cytoscape [24] was used to identify potential interaction partners of HOXB8, as discussed in [25]. Primers were designed using Primer-BLAST (https://www.ncbi.nlm.nih.gov/tools/primer-blast/), aiming for a 400–800 bp amplicon with the sgRNA binding site in the middle. The used sgRNA and primer sequences are listed in Supplementary tables 1 and 2.

2.3. Isolating, CRISPR modifying, and differentiating BM cells.

BM cells were collected by flushing femurs and tibias with PBS. Lineage negative cells (Lin-) were obtained by depleting lineage positive cells (Lin +) from the BM cells using MACS buffer (Miltenyi Biotec, #130–091-221), Lineage Cell Detection Cocktail-Biotin (Miltenyi Biotec, #130–092-613, 1:100), Anti-Biotin MicroBeads (Miltenyi Biotec, #130–090-485), and LS column (Miltenyi Biotec, #130–042-401), according to the protocol suggested by the manufacturer. Lin- cells were culture in complete RPMI medium (cRPMI) containing 20 ng/ml of SCF (PeproTech, #250–03), TPO (PeproTech, #315–14), IL-3 (PeproTech, #213–13), and IL-6 (PeproTech, #216–16) for two days. cRPMI: RPMI-1640 (Sigma-Aldrich #R0883) with 10% heat-inactivated fetal bovine serum and 1% penicillin–streptomycin-glutamine (100X, Gibco, #10378016). Cells were cultured at 37℃ in a humidified incubator with 5% CO_2 and handled in laminar flow hoods using standard sterile techniques.

The Neon Transfection System (Invitrogen, #MPK5000) was used for electroporation-based delivery of CRISPR components, following the manufacturer's instructions initially using the suggested program testing 24 different conditions. Electroporation condition #5 (Pulse voltage: 1700 V, Pulse width: 20 ms, Pulse number: 1) was subsequently used for mouse BM cells unless otherwise specified. For BM cells, typically 50–100 pmol sgRNA was delivered into 2^*10^5 cells per electroporation using the Neon 10 μL Kit (Invitrogen, #MPK1096) or 500–1000 pmol of sgRNA delivered into 2^*10^6 cells per electroporation using the Neon 100 μL Kit (Invitrogen, MPK10096). Electroporated Lin- cells were kept in culture for two days in cRPMI with cytokines before sequencing to allow for the CRISPR events to occur.

To differentiate the BM cells *in vitro*, electroporated Lin- cells were switched to indicated cytokines directly after electroporation; for macrophages, cRPMI with 100 ng/ml of M−CSF (PeproTech, #315–02) and cultured for 7 days, exchanging half the medium every 2–3 days; for dendritic cells, cRPMI with 100 ng/ml of Flt3L (Biolegend, #550706) and cultured for 9 days, with one 1:2 split after 4–5 days.

The macrophage phagocytosis assay was performed using a kit (Cayman Chemical, #600540) as suggested by the manufacturer. Briefly, differentiated macrophages (1:1 mix of control and sgRNA electroporated to achieve a balanced KO frequency) were incubated with the Latex Beads-Rabbit IgG-PE complex (1:250) in a 6 well plate with 3 ml of cRPMI for 30 min at 37 ℃. Cells were then washed gently and collected for further analysis.

2.4. Generating and culturing Hoxb8 BM cells.

The Hoxb8 cells were generated by transducing BM cells of C57BL/6 Cas9 + GFP + mice with an estrogen-inducible retroviral construct expressing HOXB8 (ER-Hoxb8, a kind gift from Mark P. Kamps, University of California, San Diego) as described [26–27]. Transduced BM cells were cultured in 1 μM β-estradiol (BE, Sigma-Aldrich, #E2758) and 25 nM mouse SCF (PeproTech, #250–03) for several weeks with HOXB8 expression turned on to establish a cell line-like population. To inactive the HOXB8 activity, BE was removed from the media for 3 days. The Hoxb8 cells were CRISPR modified in the same way as BM cells (described in 2.2–2.3.).

2.5. Culturing and modifying peripheral blood mononuclear cells (PBMC) and Jurkat cells

PBMCs were derived from buffy coats from consenting healthy donors (Karolinska Hospital Blood Bank) in line with local guidelines. PBMCs were isolated using Ficoll-Paque Plus (GE Lifesciences, #17144002) according to the manufacturer's recommended protocol. PBMCs were cultured in CTS OpTmizer (Gibco, #A1048501) with 10% heat-inactivated fetal bovine serum, 1% penicillin–streptomycin-glutamine and 25 units/mL of IL-2 (Peprotech, #200–02), exchanging half the medium every 2–3 days. To expand the T cell population, PBMCs were stimulated with CD3/28 beads (Milteny Biotech, #130–091-441), re-stimulated every 7–10 days, and analyzed by flow cytometry to confirm the percentage of T cells in the culture. When used for sgRNA electroporation, the culture was more than 90% T cells (TCR-α/β positive cells by flow cytometry).

The Jurkat-NF-κB-GFP cell line was generated by transducing Jurkat cells (ATCC, TIB-152) with the pSIRV-NF-κB-eGFP (Plasmid #118093), a gift from Peter Steinberger [28] as described in Boddul et al. [29], with the modification that Ecotropic Receptor Booster (Takara, #631471) was added to the cells as suggested by the manufacturer to enable transduction of the human cell line. The cells were maintained in cRPMI.

For both the Jurkat and PBMCs, the Neon electroporation condition #24 (Pulse voltage: 1600 V, Pulse width: 10 ms, Pulse number: 3) was used. 60 pmol of sgRNA was complexed with 10 pmol of Cas9 protein (Sigma-Aldrich, #CAS9PROT) and electroporated into $5*10^4$ Jurkat cells per reaction, and 100 pmol of sgRNA was complexed with 16 pmol of Cas9 protein and electroporated into $2*10^5$ PBMCs per reaction using the Neon Transfection System 10 μL Kit.

WT, electroporated (empty) control, and T cell receptor alpha chain constant (TRAC) sgRNA electroporated PBMCs or Jurkat cells were cultured for at least seven days before the experiment. The cells were stimulated with 100 nM PMA/Ionomycin (Sigma-Aldrich, #P8139 and #I3909) or CD3/28 beads (Milteny Biotech, #130–091-441) in a 1:1 bead to cell ratio for 18 h and the beads were removed with the MACSiMAG Separator (Milteny Biotech, 130–092-168), before analysis by flow cytometry.

2.6. Flow cytometry analysis and sorting

Single-cell suspensions were stained for 30 min, washed and sorted using Sony SH800S, or acquired using BD LSRFortessa, BD FACSVerse, BD Accuri, or Cytek Aurora. Generated FCS files were analyzed by FlowJo version 10 (FlowJo, LLC).

Lin- BM cells were stained with Sca1–PE/Cy7 (Biolegend, #108113), c-Kit–APC (BD Biosciences, #561074), Lin–biotin (Lineage Cell Detection Cocktail-Biotin, Miltenyi Biotec, #130–092-613), Streptavidin–PE (BD Biosciences, #554061) and LIVE/DEAD Fixable Aqua Dead Cell Stain Kit (Invitrogen, #L34957). B cells and T cells were sorted from *Zap70* iCR mice spleen stained with CD45.1–FITC (BD Biosciences, #561871), CD45.2–BV785 (Biolegend, #109839), TCRb–BV711 (Biolegend, #109243), B220–PE (Invitrogen, #12–0452-82) and DAPI (Sigma-Aldrich, #D9542, 0.1 μg/ml). Macrophages were stained with CD11b–PerCP/Cy5.5 (Biolegend, #101228), F4/80–PE (Biolegend, #123110), and DAPI for flow cytometry analysis, and with CD11b–PerCP/Cy5.5 (Biolegend, #101228) and F4/80–BV421 (Biolegend, #123131) for phagocytosis and cell sorting. Dendritic cells were stained with CD11c-PE-Cy7 (Biolegend, #117318), I-A/I-E-AlexaFluor 647 (Biolegend, #107617), and LIVE/DEAD Fixable Near-IR dead cell stain kit (ThermoFisher Scientific #L10119). Hoxb8 cells were stained with biotin anti-mouse Lineage Panel (BioLegend #133307), Streptavidin-BV421 (BD Biosciences, #563259), LIVE/DEAD Fixable Aqua Dead Cell Stain Kit (Invitrogen, #L34957). Samples from *GFP* iCR mice were stained with the following panels: alveolar macrophages from the lung were stained with LIVE/DEAD Fixable Aqua Dead Cell Stain Kit (Invitrogen, #L34957), CD45.1-BV605 (Biolegend, #110738), CD45.2–BV785 (Biolegend, #109839), CD11c-PE/Cy7 (BD Biosciences, #558079), F4/80-BV421 (BD Biosciences, #565411). B1 cells from the peritoneal cavity were stained with LIVE/DEAD Fixable Aqua Dead Cell Stain Kit (Invitrogen, #L34957), CD45.1-BV605 (Biolegend, #110738), CD45.2–BV785 (Biolegend, #109839), CD19-Alexa647 (Biolegend, #115522), B220-APC/Cy7 (BD Biosciences, #552094). Neutrophils from blood were stained with LIVE/DEAD Fixable Aqua Dead Cell Stain Kit (Invitrogen, #L34957), CD45.1-BV605 (Biolegend, #110738), CD45.2–BV785 (Biolegend, #109839), CD11b–PerCP/Cy5.5 (Biolegend, #101228), Ly/6G-Alexa64 (Biolegend, #127610). Germinal center B cells from Peyer's patches were stained with LIVE/DEAD Fixable Aqua Dead Cell Stain Kit (Invitrogen, #L34957), CD45.1-BV605 (Biolegend, #110738), CD45.2–BV785 (Biolegend, #109839), TCRb–BV711 (Biolegend, #109243), B220-APC/Cy7 (BD Biosciences, #552094), CD95-BV650 (BD Biosciences, #740507), Gl7-PE/Cy7 (Biolegend, #144619). To confirm TCRα knockout efficiency on Jurkat cells and PBMCs, cells were stained with TCR α/β–APC antibody (Biolegend, #306717). Stimulated Jurkat cells and PBMCs were stained with TCR α/β–APC antibody (Biolegend, #306717) CD69-PE (Biolegend, #310905), and LIVE/DEAD Fixable Aqua Dead Cell Stain Kit (Invitrogen, #L34957).

2.7. Sanger sequencing, Inference of CRISPR Edits (ICE) analysis, and indel Detection by amplicon analysis (IDAA).

At least 10,000 sorted cells or 10 μL of whole blood sample were collected for genomic DNA extraction using the DNeasy Blood & Tissue Kit (Qiagen, #69504). 3 μL of genomic DNA was used as template to amplify the sgRNA target region, using a standard PCR program. Amplicons were purified directly from the PCR reaction mix by using DNA Clean & Concentrator Kits (Zymo Research, #D4013) or recovered from agarose gels by using Zymoclean Gel DNA Recovery Kit (Zymo Research, #D4007). The PCR products were quantified by Nanodrop and sequenced by Eurofins Genomics. The Sanger sequencing data was subsequently analyzed by ICE (Synthego, https://ice.synthego.com). For the IDAA fragment length analysis, genomic DNA samples were sent to COBO Technologies (https://cobotechnologies.com/).

2.8. Statistics

Statistical tests were performed as indicated in the respective figure legend using GraphPad Prism 8.

3. Theory/calculation

Sanger sequencing can be used as a simple readout to identify the role of CRISPR-targeted genes in complex cellular behaviors.

4. Results

4.1. Lineage negative (Lin-) bone marrow (BM) cells can readily be modified by CRISPR and evaluated by sequencing.

To enable the study of the role of different genes in the hematopoietic system, we first set out to optimize methods modifying HSCs with CRISPR. To this end, we isolated BM cells from Cas9 + GFP + mice on the C57BL/6 background [30], and enriched HSCs by lineage (Lin) depletion (to eliminate mature Lin + cells). The Lin- cells were cultured in the presence of cytokines for two days and then electroporated with a *GFP* targeting sgRNA. The extent of *GFP* inactivation (KO) was analyzed by flow cytometry

(Fig. 1**A**). Screening different electroporation programs, we identified a set of parameters that gave a good KO efficiency without a substantial effect on cell survival, although some variation was seen comparing independent experiments as indicated by the error bars (Fig. 1**B, and Supplementary** Fig. 1**A-C**). We selected condition #5 (pulse voltage: 1700 V, pulse width: 20 ms, pulse numbers: 1) and further tested how the concentration of sgRNA affected the KO efficiency, identifying that doses of 50 pmol or more gave a high and uniform KO efficiency (**Supplementary** Fig. 1**D**). GFP, as well as surface markers that can be readily stained with antibodies, are easily followed by flow cytometry. However, the genotype of most genes is not easily evaluated by flow cytometry. As an alternative readout, we hypothesized that we could use standard Sanger sequencing to quantify the CRISPR-induced genotype. Using the ICE software [13] to analyze Sanger sequencing data, we observed that the used *GFP* targeting sgRNA generated a diverse genotype in the Lin- cells, with a dominant + 1 insertion next to the expected cut site (Fig. 1**C**). To compare the two methods assessing CRISPR-efficiency of gene KO, we generated a dilution curve of cells with different levels of *GFP* KO by diluting sgRNA electroporated Lin- BM cells with different proportions of non-electroporated Lin- BM cells. Sequencing of the mutation frequency was then compared to the KO phenotype identified by flow cytometry in the same cells. We found a good correlation between the two readouts (R^2 = 0.87, p = 0.0007), although the sensitivity of the sequencing readout was decreased when mutations were found at a low frequency, something that can be expected by the nature of the sequence deconvolution (Fig. 1**D**). As an alternative, we used the IDAA fragment length analysis approach and found a very strong correlation to the flow cytometry readout (R^2 = 0.99, p < 0.0001) (Fig. 1**E**). Sequencing and IDAA can thus both be used as readouts to quantify the mutation frequency when flow cytometry is not a feasible readout.

We next hypothesized that the mutation frequency of one targeted gene (*X*), could predict the mutation frequency of another gene (*Y*) in a cell population simultaneously electroporated with two sgRNAs (targeting *X* and *Y*). Such an approach is based on the idea that if a cell inactivates one gene, it has a high chance of also successfully inactivating another co-targeted gene. This type of approach could be used as a strategy to enrich for cells with the intended mutation, similar to what has been described by co-targeting *DTR* [31], or *HPRT* [32]. To this end, we electroporated the Lin- BM cells with a combination of *GFP* and *Syk* sgRNAs, sorted the GFP positive (+) and GFP negative (−) cells after two days, and sequenced the targeted *GFP* and *Syk* loci in the sorted cells (Fig. 1**F**). In line with the hypothesis, the cell population that failed to inactivate GFP (GFP + cells), had no detectable mutations in *GFP*, and only minimal mutations in *Syk* (Fig. 1**G**). We concluded that: (*i*) we had established an optimized system for modifying genes in Lin- BM cells by CRISPR, (*ii*) a simple Sanger sequencing readout could be used to quantify the mutation frequency in a cell population, albeit not when the mutations are found at a low frequency, and (*iii*) co-targeting *GFP* and a second gene of interest followed by sorting cells with inactivated GFP constitutes a strategy to enrich for mutations in the gene of interest.

4.2. Generating immuno-CRISPR (iCR) mice and evaluating the CRISPR-mediated modifications by sequencing.

We applied the optimized protocol to generate *in vivo* models with the modified Lin- BM cells. For this purpose, Lin- BM cells from Cas9 + mice were cultured and electroporated with a *Zap70* targeting sgRNA, followed by transplantation to irradiated recipients, generating what we refer to as immuno-CRISPR (iCR) mice (Fig. 2**A**). ZAP70 is a component of the T cell receptor signaling pathway essential for mature T cell development [33–34], but with a redundant role for B cell development [35]. In line with the literature related to *Zap70* deficiency, we saw a diminished T cell population in the spleen of *Zap70* iCR mice, and a corresponding increase in the frequency of B cells within the lymphocyte gate (Fig. 2**B-C**). Furthermore, after sequencing *Zap70* in sorted B and T cells from the *Zap70* iCR mice, we observed that the B cells showed a high mutation frequency, in concordance with the fact that ZAP70 is not important for B cell development. In contrast, the sorted T cells had no detectable *Zap70* mutations (Fig. 2**D**).

Occasionally, the mutation frequency achieved in CRISPR-targeted Lin- BM cells is low, and as a consequence iCR mice generated from these cells typically have a low frequency of mutations (which could be partly underestimated due to the sensitivity of the sequencing approach) and a higher level of variability between recipient mice as exemplified in Fig. 2**E-F**. We have noted that performing secondary transplantations from a single successful iCR mouse in such a situation can generate experimental groups with a uniform mutation spectrum as shown by sequencing (Fig. 2**G**), and flow cytometry (Fig. 2**H-I, and Supplementary** Fig. 2) . Importantly, this also gives an example of how an iCR mouse population can be expanded by secondary transplantation, something that is considerably faster than expanding a traditional colony of mice by breeding. We concluded that sgRNA electroporated Lin- HSCs can be grafted into irradiated recipient mice, resulting in the formation of mature immune cells carrying the intended mutation. Furthermore, the role of a targeted gene in the differentiation of mature immune cells *in vivo* can be evaluated by sequencing, comparing the genotype of different cell populations.

4.3. In vitro differentiation of CRISPR-modified BM cells into macrophages and dendritic cells.

In immunological research, immature BM cells are commonly differentiated *in vitro* into different mature myeloid immune cell populations by the addition of specific cytokines to the cell culture medium [36]. This setup allows for controlled experiments testing parameters in isolated, non-transformed, immune cells. We next investigated whether the CRISPR-modified Lin- BM cells could be differentiated *in vitro* to defined mature immune cell populations by culturing the cells in M−CSF (for macrophage differentiation), or Flt3L (for dendritic cell differentiation) (Fig. 3**A**). In the M−CSF culture, we observed a good differentiation of cells into the expected F4/80^{high} CD11b^{high} macrophage phenotype and observed a high degree of *GFP* KO efficiency (Fig. 3**B-D**), without affecting the macrophage differentiation (Fig. 3**E**). To assess whether the modified macrophages were functional, we incubated GFP sgRNA targeted macrophages (mixed 1:1 with non-targeted macrophages to have a significant proportion of both GFP + and GFP- macrophages in the population) with PE -labeled IgG-coupled beads to assess phagocytosis and found that both GFP + and GFP- macrophages bound the beads equally well, thus showing expected functionality (Fig. 3**F-G**).

Similarly, in the Flt3L-supplemented culture, we observed that the CRISPR-modified Lin- BM cells differentiated well into dendritic cells (CD11c^{high}, MHC II^{high}) and showed a good level of *GFP* KO efficiency (Fig. 3**H-I**), which did not affect the efficiency of the differentiation to dendritic cells (Fig. 3**J**). We concluded that the CRISPR-modified Lin- BM cells could be successfully differentiated into macrophages and dendritic cells, allowing for the study of cell behaviors such as phagocytosis.

4.4. Using the rapid CRISPR competitive assay (RCC) to study T-cell activation.

We explored if a genotype competition assay could be used studying genes important for T-cell activation. We optimized the

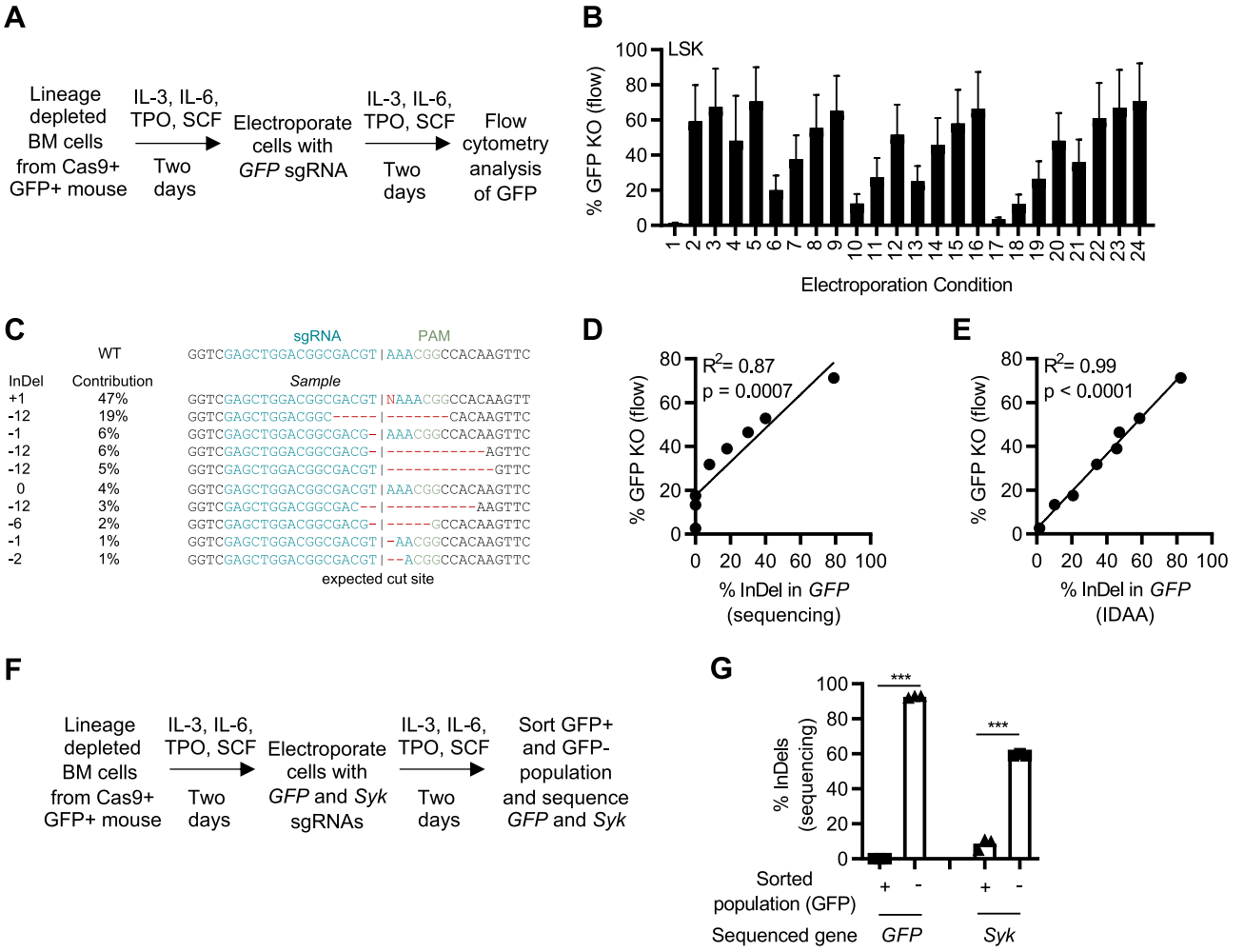

Fig. 1. Lineage negative (Lin-) bone marrow (BM) cells can readily be modified by CRISPR and evaluated by sequencing. (**A**) Model describing the experimental setup where Lin- BM cells were cultured in a cytokine cocktail, electroporated with a *GFP* targeting sgRNA, and analyzed by flow cytometry. (**B**) Flow cytometry analysis of GFP expression in Lin-, Sca1+, c-Kit+ (LSK) BM cells two days after electroporation with a *GFP* sgRNA comparing different electroporation programs. (**C**) Analysis of the sgRNA targeted *GFP* region showing the generated mutation spectrum. Data generated by the ICE software based on Sanger sequencing of PCR product. (**D**) Comparison of the identified % insertion and deletions (InDels) in *GFP* using sequencing and the % GFP KO cells by flow cytometry. (**E**) Comparison of the identified % insertion and deletions in *GFP* using the InDel Detection by Amplicon Analysis (IDAA) assay and the % GFP KO cells by flow cytometry. (**F**) Model describing simultaneously targeting *GFP* and *Syk*. (**G**) Quantification of % InDels in *GFP* and *Syk* in cells sorted by flow cytometry based on GFP expression. Data shown as mean and SEM (B, n = 4) and mean and individual values (G). *** = p < 0.001 unpaired T-test (G), and simple linear regression (D-E).

delivery of sgRNA/Cas9 complexes in Jurkat cells (a human acute T cell leukemia cell line, [37], as well as primary human T cells expanded from PBMC of healthy donors (**Supplementary** Fig. 3). Using the optimized parameters, we subsequently targeted the *LCP2* gene in the Jurkat cell line carrying an NF-κb-GFP reporter and activated the cells through the T cell receptor (TCR) with anti-CD3/28, or with the Protein kinase C (PKC) activator phorbol 12-myristate 13-acetate (PMA), which activates the cells independently of the TCR (Fig. 4**A**). We sorted activated cells, based on the GFP reporter, and identified that LCP2 plays an essential role for TCR-mediated activation, as shown by significantly lower *LCP2* mutation frequency in the successfully CD3/28 activated cells (GFP +) compared to GFP- cells (Fig. 4**B-C**). In contrast, LCP2 was dispensable for PKC-mediated PMA activation (Fig. 4**B-C**). This finding was in line with the central role for LCP2 (SLP-76) specifically in the TCR signaling pathway [38–39].

4.5. Using the RCC assay to study transformation by the HoxB8 proto-oncogene.

Lastly, we wanted to assess if our experimental setup could be used to study the role of different genes in relation to malignancies of the hematopoietic lineage. To this end, we transduced the Cas9 + GFP + BM cells with an inducible construct expressing the proto-oncogene *Hoxb8* [40–41] and electroporated them with different sgRNAs to identify the role of targeted genes for the HOXB8 transformed phenotype (Fig. 5**A**). When the activity of HOXB8 is induced, the BM cells are proliferating at a transformed Lin- phenotype (Fig. 5**B**) [27]. As such the cells show behavioral (unlimited proliferation, block in differentiation) and phenotypic (immature, Lin-) features that overlap with acute leukemia cells, as has been proposed [42–43]. In contrast, when the HOXB8 activity is turned off, the HOXB8-induced proliferation and differentiation block are eliminated, and the cells differentiate into mature, Lin+, cells with a limited lifespan (Fig. 5**C**) [27,44]. To test the experimental setup, we electroporated the HOXB8 transformed cells with a *HoxB8* sgRNA and three days later observed that approximately 50% of the cells had acquired the Lin + phenotype, expected when the activity of HOXB8 was turned off (Fig. 5**D**). We subsequently sorted the cells into Lin- and Lin + and sequenced the *Hoxb8* locus to quantify the mutation spectrum. As expected, we found that the Lin + population, which behaved as if the HOXB8 activity was turned off, showed a 100% mutation frequency in *Hoxb8* (Fig. 5**E**). To our surprise,

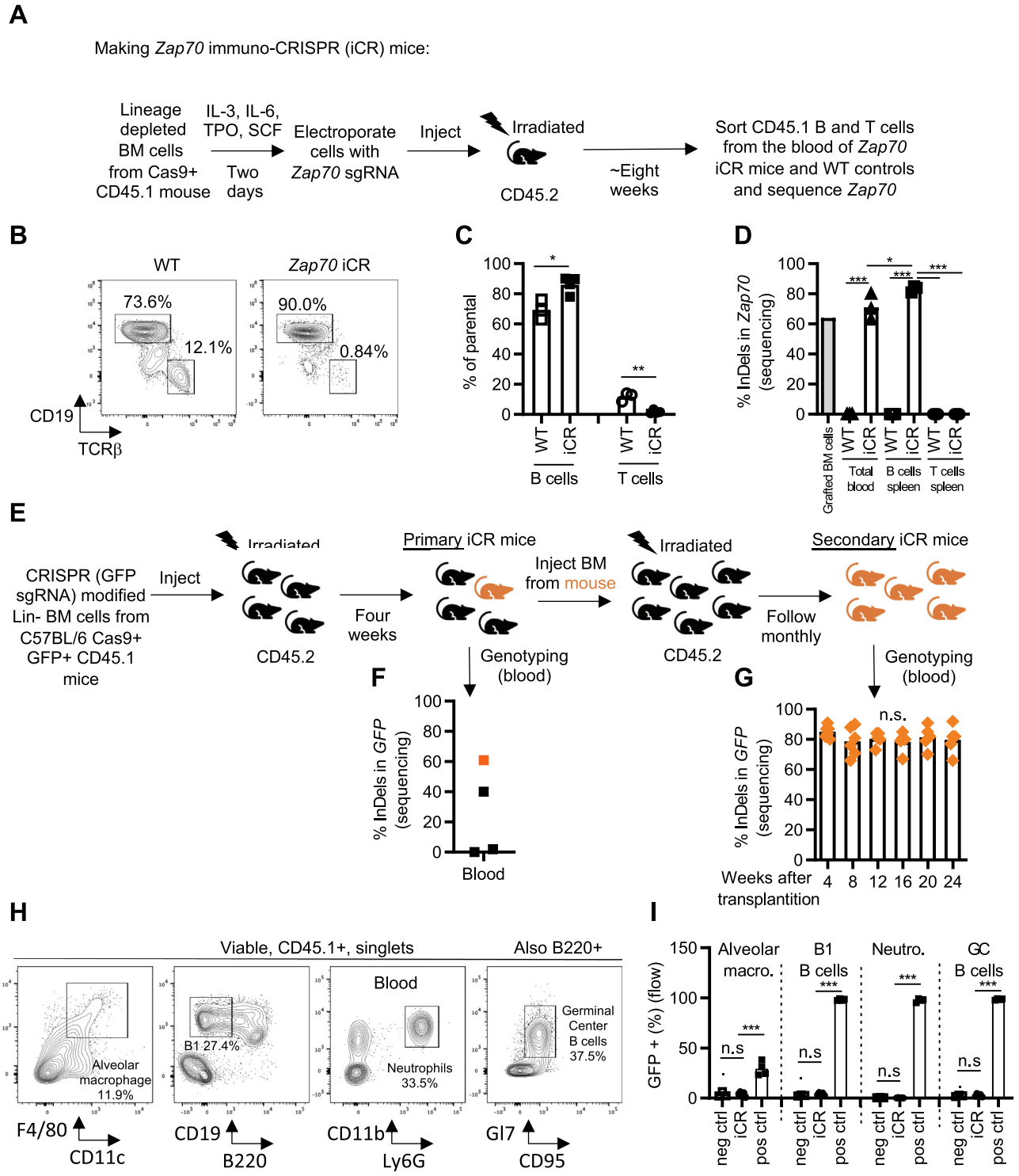

Fig. 2. Generating immuno-CRISPR (iCR) mice and evaluating the CRISPR-mediated modifications by sequencing. (**A**) Model describing the experimental setup where CD45.1 + Lin- BM cells were modified by CRISPR targeting *Zap70* and grafted into irradiated CD45.2 + recipients. (**B**) Flow cytometry analysis of cells in the blood of *Zap70* iCR mice and WT control mice eight weeks post transplantation. Cells gated on viable, CD45.1+, single lymphocytes. (**C**) Quantification of B and T cells in the blood of WT and *Zap70* iCR mice in (B). (**D**) Analysis of the level of mutations in the sgRNA targeted *Zap70* region in the BM cells used for transplantation, total cells from the blood, as well as in B and T cells sorted from the spleen of Zap70 iCR mice and WT control mice 8 weeks after engraftment. (**E**) Model describing the experimental setup where a secondary transplantation was used to amplify the population of successfully modified mice. (**F**) Analysis of the level of mutations in the sgRNA targeted *GFP* region in blood cells of the *GFP* iCR mice four weeks after transplantation, in an experiment with low efficiency. One mouse showed good knockout efficiency (labeled in orange) and was used as BM donor for secondary transplantation. (**G**) Kinetics of the level of mutations of *GFP* in the secondary iCR mice. (**H**) As examples, representative flow cytometry plots and (**I**) GFP + cell population percentage of alveolar macrophages, B1 cells, neutrophils and germinal center B cells from secondary iCR mice in G. Data shown as mean and individual data points (C-D, n = 3; F, n = 4; G-I, n = 3–6). n.s. = non-significant, * = $p < 0.05$, ** = $p < 0.01$ *** = $p < 0.001$ by unpaired T-test (C), and one-way ANOVA and Tukey's post-test (D, G, I). (For interpretation of the references to colour in this figure legend, the reader is referred to the web version of this article.)

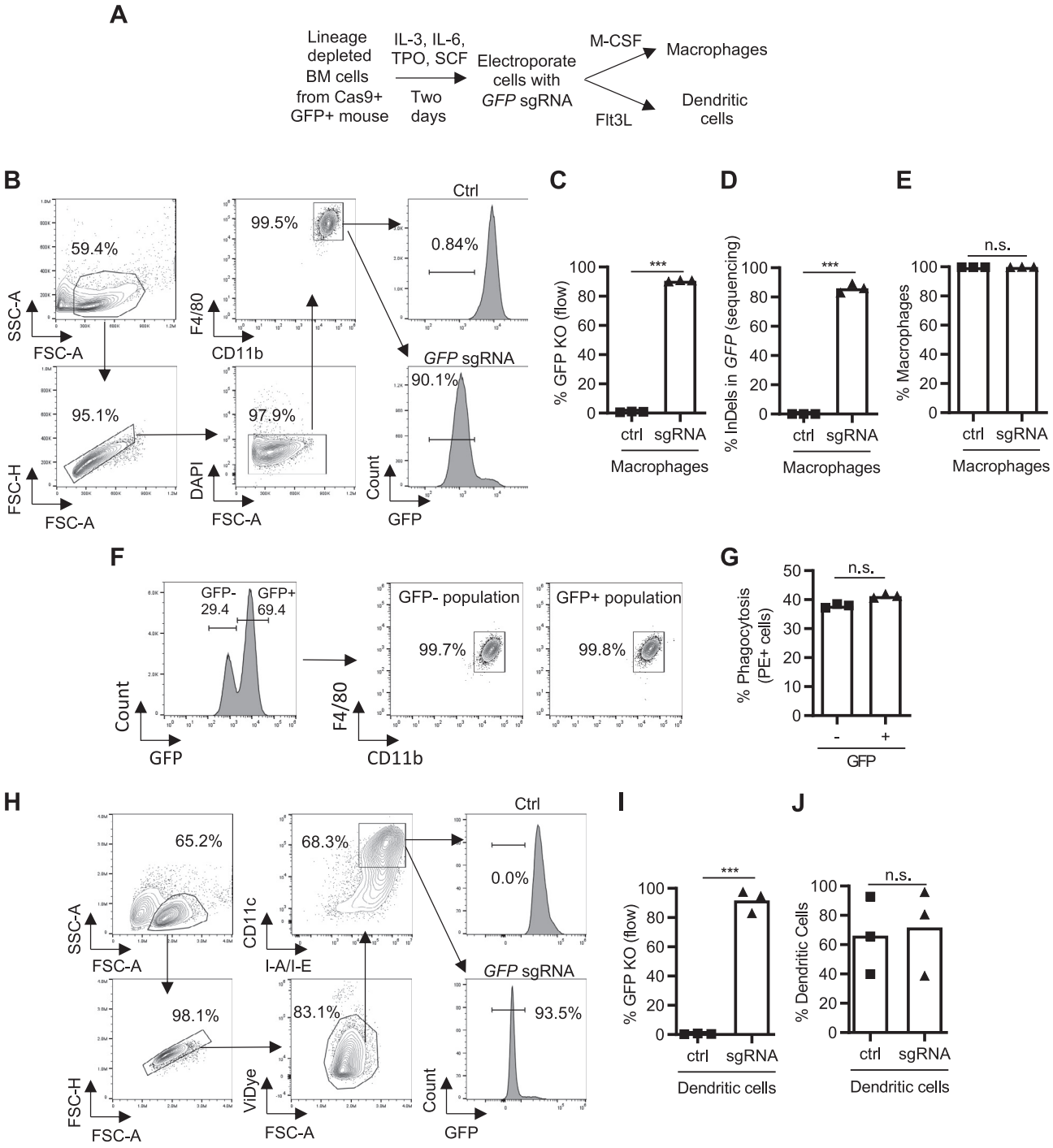

Fig. 3. ***In vitro*** **differentiation of CRISPR-modified BM cells into macrophages and dendritic cells.** (**A**) Model describing the experimental setup. (**B**) Flow cytometry plots showing the gating strategy for cells differentiated for seven days in M−CSF. *GFP* KO percentage (**C**) and InDel frequency (**D**) in sorted macrophages (viable, F4/80+, CD11b + singlets) from M−CSF cultures. (**E**) Macrophage differentiation efficiency in Lin- Cas9 + cells electroporated +/- *GFP* sgRNA. (**F**) Macrophages generated from control and *GFP* sgRNA electroporated Lin- Cas9 + BM cells were mixed 1:1, incubated with PE/IgG phagocytosis beads, and 30 mins later analyzed for binding efficiencies. Representative FACS plots shows gating for GFP + and GFP- viable singlets, followed by analysis of F4/80 and CD11b expression. (**G**) Quantification of phagocytosis efficiency (% PE +) in GFP- and GFP + macrophages. (**H**) Flow cytometry plots showing the gating strategy for Lin- Cas9 + cells electroporated +/- GFP sgRNA and then differentiated for nine days in Flt3L. (**I**) Frequency of GFP KO by flow cytometry in dendritic cells (viable, CD11c+, MHC II + [I-A/I-E +] singlets) from Flt3L cultures. (**J**) Dendritic cell differentiation efficiency in Lin- Cas9 + cells electroporated +/- GFP sgRNA. Data shown as representative flow cytometry plots (B, F, H), mean and individual data (C, D, E, G, I, J, n = 3). n.s. = non-significant, *** = $p < 0.001$ by unpaired T-test (C, D, E, G, I, J).

we also noted that the Lin- population had a significant amount of mutations in the *Hoxb8* transgene. Detailed analysis showed that these mutations almost exclusively corresponded to different insertions or deletions (InDels) with a multiplier of three nucleotides, in contrast to the Lin + population where InDels consisted of a multiplier of one or two nucleotides (Fig. 5**E-F**, and **Supplementary** Fig. 4). This is in line with the fact that an InDel with a multiplier of one or two nucleotides causes a frameshift, premature stop codons, and nonsense-mediated decay, essentially causing a KO of the gene in most cases [45–

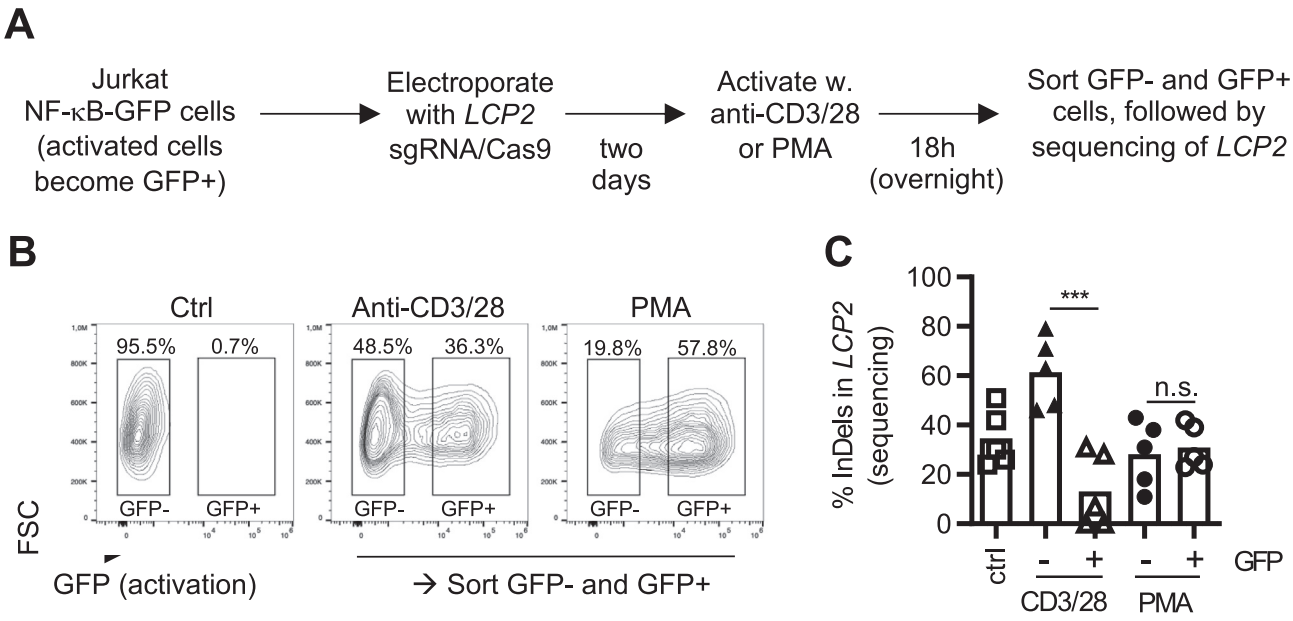

Fig. 4. Rapid identification of genes linked to T cell activation (**A**) Model describing the experimental setup where Jurkat NF-kB-GFP reporter cells were modified by an *LCP2* sgRNA. (**B**) Representative flow cytometry plots showing GFP staining of the Jurkat NF-kB-GFP cells, and sorting gates used for (C). A low PMA dose (2.5 nM) was used to allow a dynamic response including both GFP- and GFP + cells (**C**) LCP2 InDel frequency in sorted viable Jurkat cells (GFP + or GFP-) stimulated as indicated in figure. Ctrl is the whole, unsorted population. Data shown as representative flow cytometry plots (B), mean and individual data (C, n = 5). n.s. = non-significant, *** = p < 0.001 by one-way ANOVA and Tukeýs post-test (C).

46]. On the other hand, InDels with a multiplier of three nucleotides will result in the insertion or deletion of amino acids (AA) in the translated protein (**Supplementary** Fig. 4**D**), something that depending on the protein and the specific site where the change occurs, can inactivate the protein, or, as it appears to be the case here, leave the protein sufficiently functional.

Since our data indicated that we could use the experimental setup to study the role of genes influencing the transformation caused by HOXB8, we set out to test whether we could identify more genes involved in the transformed phenotype. Using geneMANIA we identified a list of proteins that physically interact with HOXB8 (Fig. 5**G**). In addition to the already used *Hoxb8* sgRNA, we also decided to target the top two identified candidate genes *Pbx1* and *Meis1* in transduced cells with active HOXB8 (+BE) keeping the cells in the immature Lin- phenotype. We found that all three sgRNA induced a good level of mutations, with a high level of frameshift mutations in the targeted cell population (Fig. 5**H**). Moreover, we observed that the *Meis1* sgRNA was able to induce the differentiation of HOXB8 transduced cells to the Lin + phenotype (Fig. 5**I**). In contrast, the *Pbx1* sgRNA did not affect the transformed Lin- phenotype despite the high level of mutations found in the cells (Fig. 5**H-I**). Sorting the Lin + cells in the *Meis1* sgRNA targeted cell population further confirmed that all identified sequences were InDels with a multiplication of one or two nucleotides, expected to generate a KO phenotype (Fig. 5**J**). We concluded that the presented experimental setup is suitable to study genes affecting the transformed state of a leukemia-like cell population and that Sanger sequencing can be used as a simple readout to evaluate the experiment.

5. Discussion

Comparisons of WT and KO cells are a fundament for experimental research to dissect the role of specific genes in a given biological context. Traditionally, generating KO alleles have involved time-consuming and expensive homologous recombination techniques [47]. With the development of flexible, sequence-specific nucleases, including CRISPR, this process has been dramatically simplified [48]. However, the resulting genotype in a CRISPR-targeted cell population is not uniform, as exemplified in Fig. 1C . With a binary mindset (e.g. WT or KO), the analysis of a CRISPR-targeted population could thus be non-productive. Often, researchers address the CRISPR-created genetic heterogeneity by generating clonal lines of the targeted cells or animals. This is, however, not always possible and can result in the selection of traits that are not directly linked to the intended genotype, as well as being time consuming. Instead of identifying the CRISPR-induced genetic heterogeneity as a problem, we hypothesized that the heterogeneity could be embraced for discovery, and that Sanger sequencing could be used as a simple readout to quantify the heterogeneity and identify genotype enrichment. For this purpose, genomic DNA was isolated from the cells, and the CRISPR-targeted region was amplified by PCR and sequenced by a standard Sanger sequencing approach followed by analysis of the sequencing result file with the free web-based software ICE, which has been benchmarked to next-generation sequencing in Hsiau et al. [13]. Delivering a *GFP* targeting sgRNA into the Lin- BM cells, isolated from Cas9 + GFP + mice, we compared a flow cytometry-based assay for *GFP* inactivation to the sequencing of the targeted *GFP* locus. We found that the readouts showed a good correlation (R^2 = 0.87), although the sequencing readout had a lower sensitivity when the mutations were found at a low frequency (Fig. 1D). This could be expected based on the way ICE analyzes the samples, where the mixed peaks of the sequencing readout are deconvoluted into frequencies, with low-frequency mutations being more difficult to resolve. As an alternative readout, we used the same genomic DNA samples and the same primers to perform fragment length analysis (FLA) using the IDAA technology [11–12]. This approach separates the PCR product by capillary electrophoresis and in a precise way defines the size of the different products formed in the PCR reaction. This approach is not constrained by the same type of sensitivity issues as the sequence deconvolution

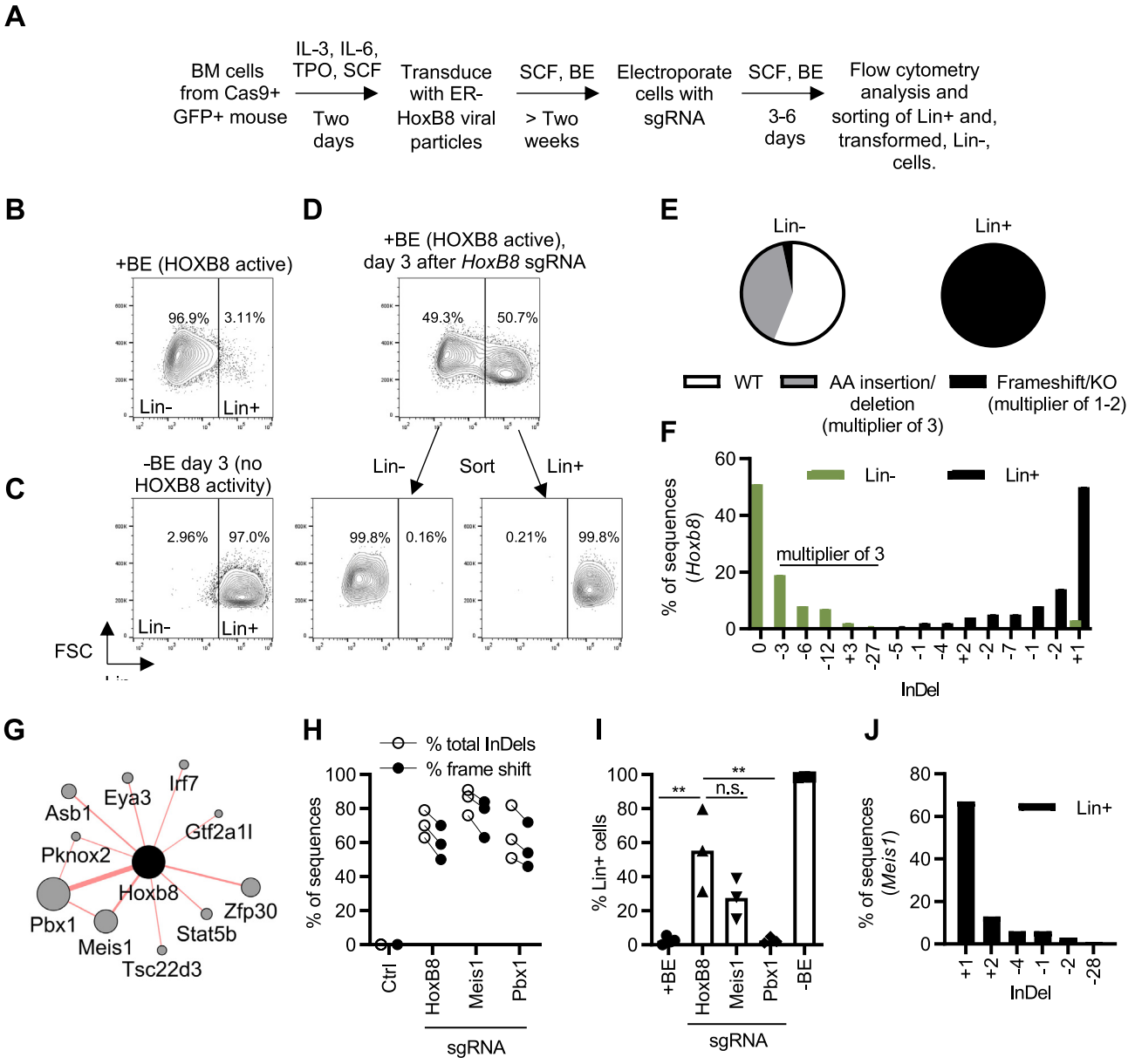

Fig. 5. Using the Rapid CRISPR Competitive Assay (RCC) to study transformation by the *Hoxb8* proto-oncogene. (**A**) Model describing the experimental setup where Cas9 + BM cells were transduced with Estrogen Receptor (ER)-Hoxb8 retroviral particles. HOXB8 in the transduced cells is activated by the addition of b-estradiol (BE), resulting in proliferation and block of differentiation at an immature Lin- stage. The cells were subsequently electroporated with different sgRNAs to identify genes affecting the transformed, Lin-, phenotype. (**B-C**) Flow cytometry analysis of ER-Hoxb8 BM cells in the presence (B), or absence of BE (C). (**D**) Sorting of Lin- and Lin + ER-Hoxb8 BM cells three days after electroporation with a *Hoxb8* sgRNA. (**E**) Sequencing of the sgRNA targeted *Hoxb8* locus, and deconvolution of mutation spectrum using ICE. Data shows the % of different InDels identified in the Lin- (green) and Lin+ (black) sorted cells. (**F**) Proportions of mutations found in sorted Lin- and Lin + populations; WT (no InDels), amino acid (AA) insertion/deletion (InDels with a multiplier of 3 nucleotides, resulting in the addition or removal of amino acids), Frameshift/KO (InDels with a multiplier of 1 or 2 nucleotides, resulting in a frameshift, and introduction of premature stop codon). (**G**) Top physical interaction partners of HOXB8 identified by geneMANIA. The size of the circle indicates the level of identified interactions, where the larger circles represent more prominent interaction partners. (**H-I**) The ER-HoxB8 BM cells were cultured in BE, to keep HOXB8 active, electroporated with indicated sgRNAs, and sequenced to quantify the level of induced mutations (H), as well as analyzed by flow cytometry for Lin expression (% Lin + cells) after 3 or 6 days (three independent experiments represented in the graphs) (I). (**J**) Genotype of the CRISPR-targeted *Meis1* region in sorted Lin + cells from Meis1 sgRNA electroporated cells. Data shown as individual data points (F; H, J), or mean and individual data points (I). n.s. = non-significant, ** = $p < 0.01$ by one-way ANOVA and Tukey's post-test (I). (For interpretation of the references to colour in this figure legend, the reader is referred to the web version of this article.)

approach and showed a great correlation (R^2 = 0.99) to the flow cytometry-based readout (Fig. 1E). Based on the simplicity, speed, and cost-effectiveness of the Sanger sequencing approach, we have continued to use this readout, keeping in mind the limitation of detection at low mutation frequencies. Notably, since the same genomic DNA samples and primers can be used for the FLA assay, important samples can be analyzed first by the Sanger sequencing approach and subsequently by FLA if necessary. NGS-based readouts can also be considered, and several amplicon-based analysis pipelines are established for analyzing CRISPR targets [8–10].

As we had optimized culture conditions and sgRNA delivery to mouse Lin- BM cells, we next performed a set of experiments to assess the discovery potential using Sanger sequencing as a readout. Conceptually, the idea was to let cells with different genotypes compete and see if specific genotypes were enriched when studying different cellular behaviors or phenotypes. We refer to this

setup as the rapid CRISPR competitive (RCC) assay. Notably, in many ways, the RCC assay exploits the same fundamental mechanisms as a CRISPR screen but focuses on one gene (that is Sanger sequenced), instead of a set of genes (where sgRNA barcodes are sequenced by NGS in the screen setting). To this end, we first tested if the approach could be used to identify genes that affect the development of immune cells *in vivo*. We electroporated the Lin- BM cells (GFP + Cas9 + CD45.1 +) with a *Zap70* sgRNA and transferred them into irradiated CD45.2+ (GFP + Cas9 + CD45.2 +) recipient mice. In the recipient mice, the transferred, modified BM cells graft into the BM compartment and start generating new immune cells that can be tracked by the CD45.1 expression. We refer to these mice as immuno-CRISPR (iCR) mice. *Zap70* was selected as a proof-of-concept target, as it is known to be essential for T cell development, while not affecting for example B cell development [33–35]. As anticipated, we found that sorted CD45.1 + B cells had a high proportion of mutations in *Zap70*, while we could not detect any mutations in CD45.1 + T cells in the *Zap70* iCR mice (Fig. 2D). Hence, the RCC assay worked well to evaluate the role of *Zap70 in vivo*. Considering the complexity and cost of generating gene-modified mice, even with novel CRISPR-based approaches, we see great potential in using the iCR approach to rapidly study the role of different candidate genes in mature immune cells and hematopoiesis. This approach shares similarities with mixed BM chimera experiments, but instead of using flow cytometry to identify the enrichment/depletion of cells with specific congenic markers (used as a proxy for a specific genotype), sequencing is directly used to identify the enrichment/depletion of specific genotypes. In line with the *in vivo* differentiation data, we also found that the modified Lin- BM cells could be readily differentiated *in vitro* into both macrophages and dendritic cells with an expected phenotype (Fig. 3). Furthermore, we found that the RCC assay could be used to identify genes affecting T cell activation *in vitro* (Fig. 4 and Supplementary Fig. 3)

Lastly, we explored whether our analysis pipeline could also be used to study malignant transformation induced by the overexpression of a proto-oncogene linked to leukemia [27,43–44]. We induced the activity of HOXB8 in BM cells, resulting in a transformed state characterized by the cells proliferating at an immature (Lin-), leukemia-like, differentiation stage [27]. Subsequently, we evaluated cell differentiation into the mature (Lin +) non-transformed state as cells were electroporated with different sgRNAs, aiming to identify potential drug targets affecting the transformed phenotype. Initially, we targeted *Hoxb8* itself as a proof-of-concept. We found that half of the CRISPR-targeted cells lost the leukemia-like phenotype and differentiated to a mature (Lin +) cell state, defined by expected inactivating mutations in the *Hoxb8* region (Fig. 5D-F, and Supplementary Fig. 4). Interestingly, we also found that the Lin- population had a reasonable amount of mutations, despite retaining the HOXB8-induced transformed phenotype at the tested timepoint (Fig. 5E-F, and Supplementary Fig. 4). By closer examination, we noted that the mutations found in the Lin- population were mainly −3, −6, and −12 nucleotides, corresponding to the deletion of 1, 2, and 4 AAs, respectively. Conversely, in the Lin + population we found a dominant + 1 mutation, followed by less abundant −2, −1, −7, −2, +2, −4 and −1 mutations, all being frameshift mutations resulting in premature stop codons, and nonsense-mediated decay [45–46]. This observation suggests that the deleted/mutated AAs in the Lin- population, located approximately 70 AAs upstream of the DNA-binding Homeobox domain (Supplementary Fig. 4A), in a region with no defined structure, are not essential for the HOXB8 activity required to maintain the Lin- phenotype. Arguably, such a phenomenon can be expected to be very protein and target specific. For example, we see no evidence for such phenomenon with the used *GFP* sgRNA, where sorted GFP + cells in a population targeted by the *GFP* sgRNA, had no detectable InDels (Fig. 1G). Nevertheless, the *Hoxb8* data (Fig. 5E-F) identified that comparing the frequency of total InDels to the frequency of InDels expected to result in a KO phenotype (insertion/deletion with a multiplier of 1–2 nucleotides; frameshift) could be a way to identify protein domains with structural and functional significance. The discovery potential of this approach, however, needs to be validated at a larger scale.

The lack of effect by knocking out *Pbx1* in HOXB8 overexpressing cells (Fig. 5I) was surprising as the PBX1 binding site in HOXB8 has been reported to be important for most, but not all, features of HOXB8 overexpression in experimental systems [44]. However, our data is in line with CRISPR screen data from HOXB8 overexpressing cells, identifying that *Hoxb8*, and *Meis1*, but not *Pbx1*, sgRNAs are depleted over time, further supporting our observations [49]. One possible explanation is that the activity of PBX1 is redundant, and that other PBX proteins could perform the same task, like PBX3 as described in Knoepfler *et* al. [44]. Notably, this type of CRISPR experimental approach is not able to resolve the specific biological question related to the role of different members of the PBX family. However, it shows that PBX1 targeting is likely not a relevant therapeutic target to suppress HOXB8-mediated transformation, while MEIS1 targeting in contrast could be an interesting candidate target.

The concept of comparing cells or microorganisms with different genotypes in competitive settings is a proven discovery model. It is, for example, the basis for CRISPR and shRNA screens, as well as for mixed BM chimera experiments. The same "survival of the fittest" mechanisms is furthermore the basis for the enrichment of specific mutations in cancer cells and infectious agents, both spontaneously over time and in response to drugs [50–53]. The enrichment of specific genotypes in all these settings infers a central functionality to the specific genotypes and can thereby guide the development of drug candidates targeting the identified genes/proteins. Here, we set out to establish a simple experimental setup to identify the role of different genes in studied cellular behaviors. We use standard Sanger sequencing to quantify the genetic diversity induced at a CRISPR-targeted site and successfully use enrichment of specific genotypes to identify the role of the studied gene.

6. Conclusions

Sanger sequencing and sequence deconvolution can be used as a rapid and cheap discovery readout to identify the role of CRISPR-targeted genes *in vitro* and *in vivo*.

Declaration of Competing Interest

The authors declare that they have no known competing financial interests or personal relationships that could have appeared to influence the work reported in this paper.

Acknowledgements

We are grateful to Drs. Helena Malmgren, Lisa Westerberg, Taras Kreslavskiy, Laura Plant and Sudeepta Panda for valuable discussions and input. The ER-Hoxb8 construct was a gift from Mark P. Kamps, University of California, San Diego. The pSIRV-NF-κB-eGFP construct was a gift from Peter Steinberger, Medical University of Vienna. This research was partly funded by grants from the Swedish Research Council, the Swedish Cancer Society, Karolinska Institutet, Magnus Bergvalls stiftelse, Stiftelsen Professor Nanna Svartz fond, Felix Mindus contribution to Leukemia Research (to FW), the China Scholarship Council (to LJ and YS), and the Nanyang

Technological University–Karolinska Institutet Joint PhD Programme (to VSI).

Appendix A. Supplementary data

Supplementary data to this article can be found online at https://doi.org/10.1016/j.csbj.2021.09.020.

References

[1] Cong L, Ran FA, Cox D, Lin S, Barretto R, Habib N, et al. Multiplex genome engineering using CRISPR/Cas systems. Science 2013;339(6121):819–23.
[2] Jinek M, Chylinski K, Fonfara I, Hauer M, Doudna JA, Charpentier E. A programmable dual-RNA-guided DNA endonuclease in adaptive bacterial immunity. Science 2012;337(6096):816–21.
[3] Mali P, Yang L, Esvelt KM, Aach J, Guell M, DiCarlo JE, et al. RNA-guided human genome engineering via Cas9. Science 2013;339(6121):823–6.
[4] Makarova KS, Wolf YI, Iranzo J, Shmakov SA, Alkhnbashi OS, Brouns SJJ, et al. Evolutionary classification of CRISPR-Cas systems: a burst of class 2 and derived variants. Nat Rev Microbiol 2020;18(2):67–83.
[5] Hendel A, Bak RO, Clark JT, Kennedy AB, Ryan DE, Roy S, et al. Chemically modified guide RNAs enhance CRISPR-Cas genome editing in human primary cells. Nat Biotechnol 2015;33(9):985–9.
[6] Chu VT, Weber T, Wefers B, Wurst W, Sander S, Rajewsky K, et al. Increasing the efficiency of homology-directed repair for CRISPR-Cas9-induced precise gene editing in mammalian cells. Nat Biotechnol 2015;33(5):543–8.
[7] Symington LS, Gautier J. Double-strand break end resection and repair pathway choice. Annu Rev Genet 2011;45(1):247–71.
[8] Pinello L, Canver MC, Hoban MD, Orkin SH, Kohn DB, Bauer DE, et al. Analyzing CRISPR genome-editing experiments with CRISPResso. Nat Biotechnol 2016;34(7):695–7.
[9] Lindsay H, Burger A, Biyong B, Felker A, Hess C, Zaugg J, et al. CrispRVariants charts the mutation spectrum of genome engineering experiments. Nat Biotechnol 2016;34(7):701–2.
[10] Labun K, Guo X, Chavez A, Church G, Gagnon JA, Valen E. Accurate analysis of genuine CRISPR editing events with ampliCan. Genome Res 2019;29(5):843–7.
[11] Lonowski LA, Narimatsu Y, Riaz A, Delay CE, Yang Z, Niola F, et al. Genome editing using FACS enrichment of nuclease-expressing cells and indel detection by amplicon analysis. Nat Protoc 2017;12(3):581–603.
[12] Bennett EP, Petersen BL, Johansen IE, Niu Y, Yang Z, Chamberlain CA, et al. INDEL detection, the 'Achilles heel' of precise genome editing: a survey of methods for accurate profiling of gene editing induced indels. Nucleic Acids Res 2020;48(21):11958-81.
[13] Hsiau T, Maures T, Waite K, Yang J, Kelso R, Holden K, et al. Inference of CRISPR Edits from Sanger Trace Data. bioRxiv 2018:251082.
[14] Brinkman EK, van Steensel B. Rapid Quantitative Evaluation of CRISPR Genome Editing by TIDE and TIDER. Methods Mol Biol 2019;1961:29–44.
[15] Spangrude G, Heimfeld S, Weissman I. Purification and characterization of mouse hematopoietic stem cells. Science 1988;241(4861):58–62.
[16] Giladi A, Paul F, Herzog Y, Lubling Y, Weiner A, Yofe I, et al. Single-cell characterization of haematopoietic progenitors and their trajectories in homeostasis and perturbed haematopoiesis. Nat Cell Biol 2018;20(7):836–46.
[17] Jacobsen SEW, Nerlov C. Haematopoiesis in the era of advanced single-cell technologies. Nat Cell Biol 2019;21(1):2–8.
[18] Orkin SH, Zon LI. Hematopoiesis: an evolving paradigm for stem cell biology. Cell 2008;132(4):631–44.
[19] Ward E, DeSantis C, Robbins A, Kohler B, Jemal A. Childhood and adolescent cancer statistics, 2014. CA Cancer J Clin 2014;64(2):83–103.
[20] Fitzmaurice C, Dicker D, Pain A, Hamavid H, Moradi-Lakeh M, MacIntyre MF, et al. The Global Burden of Cancer 2013. JAMA Oncol. 2015;1(4):505. https://doi.org/10.1001/jamaoncol.2015.0735.
[21] Urso P, Congdon CC. The effect of the amount of isologous bone marrow injected on the recovery of hematopoietic organs, survival and body weight after lethal irradiation injury in mice. Blood 1957;12(3):251–60.
[22] Thomas ED, Lochte HL, Lu WC, Ferrebee JW. Intravenous infusion of bone marrow in patients receiving radiation and chemotherapy. N Engl J Med 1957;257(11):491–6.
[23] Doench JG, Fusi N, Sullender M, Hegde M, Vaimberg EW, Donovan KF, et al. Optimized sgRNA design to maximize activity and minimize off-target effects of CRISPR-Cas9. Nat Biotechnol 2016;34(2):184–91.
[24] Montojo J, Zuberi K, Rodriguez H, Kazi F, Wright G, Donaldson SL, et al. GeneMANIA Cytoscape plugin: fast gene function predictions on the desktop. Bioinformatics 2010;26(22):2927–8.
[25] Iyer VS, Jiang L, Shen Y, Boddul SV, Panda SK, Kasza Z, et al. Designing custom CRISPR libraries for hypothesis-driven drug target discovery. Comput Struct Biotechnol J 2020;18:2237–46.
[26] Panda SK, Wigerblad G, Jiang L, Jimenez-Andrade Y, Iyer VS, Shen Y, et al. IL-4 controls activated neutrophil FcgammaR2b expression and migration into inflamed joints. Proc Natl Acad Sci U S A. 2020;117(6):3103–13.
[27] Wang GG, Calvo KR, Pasillas MP, Sykes DB, Häcker H, Kamps MP. Quantitative production of macrophages or neutrophils ex vivo using conditional Hoxb8. Nat Methods 2006;3(4):287–93.
[28] Jutz S, Leitner J, Schmetterer K, Doel-Perez I, Majdic O, Grabmeier-Pfistershammer K, et al. Assessment of costimulation and coinhibition in a triple parameter T cell reporter line: Simultaneous measurement of NF-kappaB, NFAT and AP-1. J Immunol Methods 2016;430:10–20.
[29] Boddul SVSR, Dubnovitsky A, Raposo B, Gerstner C, Shen Y, Iyer VS, et al. In vitro and ex vitro functional characterization of human HLA-DRB1*04 restricted T cell receptors. Journal of Translational. Autoimmunity. 2021 (accepted)..
[30] Platt R, Chen S, Zhou Y, Yim M, Swiech L, Kempton H, et al. CRISPR-Cas9 knockin mice for genome editing and cancer modeling. Cell 2014;159(2):440–55.
[31] Li S, Akrap N, Cerboni S, Porritt MJ, Wimberger S, Lundin A, et al. Universal toxin-based selection for precise genome engineering in human cells. Nat Commun 2021;12(1). https://doi.org/10.1038/s41467-020-20810-z.
[32] Liao S, Tammaro M, Yan H. Enriching CRISPR-Cas9 targeted cells by co-targeting the HPRT gene. Nucleic Acids Res 2015;43(20):e134.
[33] Chan AC, Irving BA, Fraser JD, Weiss A. The zeta chain is associated with a tyrosine kinase and upon T-cell antigen receptor stimulation associates with ZAP-70, a 70-kDa tyrosine phosphoprotein. Proc Natl Acad Sci U S A. 1991;88(20):9166–70.
[34] Negishi I, Motoyama N, Nakayama K-I, Nakayama K, Senju S, Hatakeyama S, et al. Essential role for ZAP-70 in both positive and negative selection of thymocytes. Nature 1995;376(6539):435–8.
[35] Fallah-Arani F, Schweighoffer E, Vanes L, Tybulewicz VJ. Redundant role for Zap70 in B cell development and activation. Eur J Immunol 2008;38(6):1721–33.
[36] Groopman JE, Molina J-M, Scadden DT. Hematopoietic growth factors. Biology and clinical applications. N Engl J Med 1989;321(21):1449–59.
[37] Schneider U, Schwenk H-U, Bornkamm G. Characterization of EBV-genome negative "null" and "T" cell lines derived from children with acute lymphoblastic leukemia and leukemic transformed non-Hodgkin lymphoma. Int J Cancer 1977;19(5):621–6.
[38] Jackman JK, Motto DG, Sun Q, Tanemoto M, Turck CW, Peltz GA, et al. Molecular cloning of SLP-76, a 76-kDa tyrosine phosphoprotein associated with Grb2 in T cells. J Biol Chem 1995;270(13):7029–32.
[39] Shifrut E, Carnevale J, Tobin V, Roth TL, Woo JM, Bui CT, et al. Genome-wide CRISPR Screens in Primary Human T Cells Reveal Key Regulators of Immune Function. Cell 2018;175(7):1958–1971.e15.
[40] Ying Y, Wang Y, Huang X, Sun Y, Zhang J, Li M, et al. Oncogenic HOXB8 is driven by MYC-regulated super-enhancer and potentiates colorectal cancer invasiveness via BACH1. Oncogene 2020;39(5):1004–17.
[41] Alharbi RA, Pettengell R, Pandha HS, Morgan R. The role of HOX genes in normal hematopoiesis and acute leukemia. Leukemia 2013;27(5):1000–8.
[42] Goardon N, Marchi E, Atzberger A, Quek L, Schuh A, Soneji S, et al. Coexistence of LMPP-like and GMP-like leukemia stem cells in acute myeloid leukemia. Cancer Cell 2011;19(1):138–52.
[43] Salmanidis M, Brumatti G, Narayan N, Green BD, van den Bergen JA, Sandow JJ, et al. Hoxb8 regulates expression of microRNAs to control cell death and differentiation. Cell Death Differ 2013;20(10):1370–80.
[44] Knoepfler PS, Sykes DB, Pasillas M, Kamps MP. HoxB8 requires its Pbx-interaction motif to block differentiation of primary myeloid progenitors and of most cell line models of myeloid differentiation. Oncogene 2001;20(39):5440–8.
[45] Hsu P, Lander E, Zhang F. Development and applications of CRISPR-Cas9 for genome engineering. Cell 2014;157(6):1262–78.
[46] Lykke-Andersen S, Jensen TH. Nonsense-mediated mRNA decay: an intricate machinery that shapes transcriptomes. Nat Rev Mol Cell Biol 2015;16(11):665–77.
[47] Mortensen R. Overview of Gene Targeting by Homologous Recombination. Curr Protoco Mol Biol 2006;76(1). https://doi.org/10.1002/0471142727.2006.76.issue-110.1002/0471142727.mb2301s76.
[48] Gaj T, Gersbach CA, Barbas CF. ZFN, TALEN, and CRISPR/Cas-based methods for genome engineering. Trends Biotechnol 2013;31(7):397–405.
[49] Basilico S, Wang X, Kennedy A, Tzelepis K, Giotopoulos G, Kinston SJ, et al. Dissecting the early steps of MLL induced leukaemogenic transformation using a mouse model of AML. Nat Commun 2020;11(1). https://doi.org/10.1038/s41467-020-15220-0.
[50] Xie M, Lu C, Wang J, McLellan MD, Johnson KJ, Wendl MC, et al. Age-related mutations associated with clonal hematopoietic expansion and malignancies. Nat Med 2014;20(12):1472–8.
[51] Nowell P. The clonal evolution of tumor cell populations. Science 1976;194(4260):23–8.
[52] Weisblum Y, Schmidt F, Zhang F, DaSilva J, Poston D, Lorenzi JC, et al. Escape from neutralizing antibodies by SARS-CoV-2 spike protein variants. Elife. 2020;9.
[53] Klein F, Halper-Stromberg A, Horwitz JA, Gruell H, Scheid JF, Bournazos S, et al. HIV therapy by a combination of broadly neutralizing antibodies in humanized mice. Nature 2012;492(7427):118–22.